Organic Sensitizers Featuring a Planar Indeno[1,2-b]-thiophene for Efficient Dye-Sensitized Solar Cells

Kimin Lim,[a] Myung Jong Ju,[b] Juman Song,[a] In Taek Choi,[b] Kwangsuk Do,[a] Hyeju Choi,[a] Kihyung Song,[c] Hwan Kyu Kim,[b] and Jaejung Ko*[a]

An efficient organic sensitizer (JK-306) featuring a planar indeno[1,2-b]thiophene as the π-linker of a bridging unit for dye-sensitized solar cells (DSSCs) was synthesized. The sensitizer had a strong molar absorption coefficient and a red-shifted absorption band compared with JK-305, which resulted in a significant increase in the short-circuit photocurrent density. We incorporated a highly congested bulky amino group into the 2′,4′-dihexyloxybiphenyl-4-yl moiety, an electron donor, to diminish the charge recombination and to prevent aggregation of the sensitizer. Under standard AM 1.5G solar conditions, JK-306-sensitized cells in the presence of co-adsorbents cheno-

deoxycholic acid (CDCA) and 4-[bis(9,9-dimethyl-9H-fluoren-2-yl)amino]benzoic acid (HC-A), which afforded an overall conversion efficiency of 8.37% and 8.52%, respectively. Upon changing the I⁻/I₃⁻ electrolyte to the Co^II/Co^III redox couple, the cell gave rise to a significantly improved conversion efficiency of 10.02% with the multifunctional HC-A, which is one of the highest values reported for DSSCs with a cobalt-based electrolyte. Furthermore, the JK-306-based solar cell with a polymer gel electrolyte revealed a high conversion efficiency of 7.61%, which is one of the highest values for cells based on organic sensitizers.

Introduction

Dye-sensitized solar cells (DSSCs) have received intensive attention owing to low-cost fabrication and high power-conversion efficiency.[1] They provide a technically and economically promising alternative to traditional silicon based p–n junction photovoltaic devices.[2] In these cells, the sensitizer is one of the key components. DSSCs with polypyridyl ruthenium sensitizers have shown the highest efficiencies (> 11%).[3,4] A recent study has focused on metal-free organic sensitizers because of their advantages over ruthenium sensitizers, such as strong molar absorption coefficient, ease of molecular tailoring, and low material cost. Nevertheless, many organic sensitizers have still presented a low conversion efficiency and low stability. Two major factors for the low efficiency of organic DSSCs are the formation of dye aggregation on the TiO₂ surface[5,6] and interfacial charge recombination.[7–9] Several strategies have been considered for addressing both these issues such as the use of β-cyclodextrin-encapsulated molecules,[10] the structural

modification of the sensitizers,[11] and the use of additives.[12] Our concept toward a high photovoltaic performance with organic DSSCs is based on the interface engineering of a dye-adsorbed TiO₂ surface controlled by the structural modification of the sensitizer to diminish the charge recombination and to prevent the aggregation of sensitizers. The highly efficient organic sensitizers have a push–pull structure composed of a donor, conjugated bridge, and acceptor. In addition to the electron donor and acceptor units in a push–pull dye, the π-conjugated linker is of importance in improving the cell performance. A successful molecular engineering for the high efficiency was achieved by incorporating planar units, such as cyclopentadithiophene,[13–15] dithienosilole,[16,17] carbon-bridged phenylenevinylene,[18] indacenodithiophene,[19] cyclopenta[1,2-b:4,5-b′]dithiophene[2′,1′:4,5]thieno[2,3-d]thiophene,[20] and indeno[1,2-b]thiophene bridging group,[21] into the π-linker unit. In addition, the co-adsorption of dyes with additives, such as decylphosophonic acid,[22] dineohexyl bis(3,3-dimethyl-butyl)phosphinic acid,[23] chenodeoxycholic acid (CDCA),[24] and 4-[bis(9,9-dimethyl-9H-fluoren-2-yl)amino]benzoic acid (HC-A),[25–27] is proven to be effective in dissociating π–π stacking or dye aggregation. Herein, we report the usage of new organic sensitizers (JK-305 and JK-306, Figure 1) containing the bis(2′,4′-dihexyloxybiphenyl-4-yl)amino moiety as an electron donor and cyanoacrylic acid as an electron acceptor bridged by a planar indeno[1,2-b]thiophene unit as well as the co-adsorbent effect in conjunction with I⁻/I₃⁻ and Co^II/Co^III redox couples.

[a] K. Lim,+ J. Song, K. Do, H. Choi, Prof. J. Ko
Photovoltaic Materials, Department of Material Chemistry
Korea University 2511 Sejong-Ro, Sejong 339-700 (South Korea)
Fax: (+82) 44-867-5396
E-mail: jko@korea.ac.kr

[b] Dr. M. J. Ju,+ I. T. Choi, Prof. H. K. Kim
Global GET-Future Laboratory, Department of Materials Chemistry
Korea University, 2511 Sejong-Ro, Sejong 339-700 (South Korea)

[c] Prof. K. Song
Department of Chemistry, Korea National University of Education
Cheongwon, Chungbuk 363-791 (South Korea)

[+] These authors contributed equally to this work.

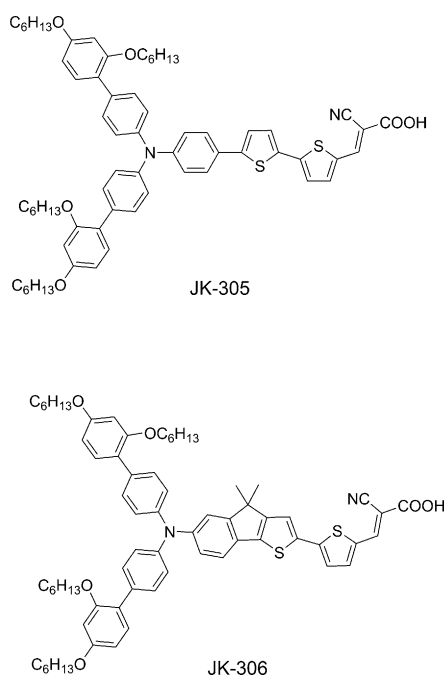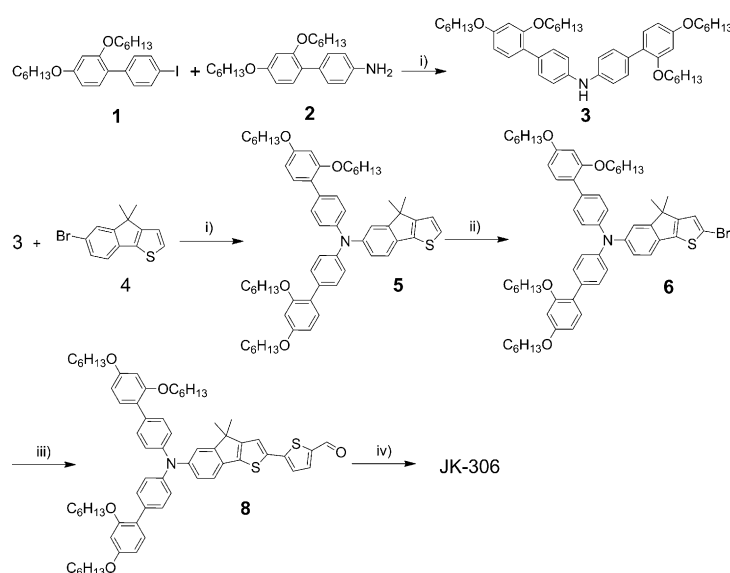Supporting Information for this article is available on the WWW under
http://dx.doi.org/10.1002/cssc.201300281.

Figure 1. Structure of JK-305 and JK-306 dyes.

Results and Discussion

Synthesis of the sensitizer

The procedures to synthesize the organic sensitizer JK-306 starting from a bis(2′,4′-dihexyloxybiphenyl-4-yl)amine (**3**) that is synthesized from the reaction of 2,4-bis(hexyloxy)-4′-iodobiphenyl (**1**) and 2′,4′-bis(hexyloxy)biphenyl-4-amine (**2**) are shown in Scheme 1. The *N*-phenylation of bromo-4,4-dimethyl-4*H*-indeno[1,2-*b*]thiophene (**4**) was performed under the Buchwald reaction conditions,[28] followed by bromination with

N-bromosuccinimide (NBS). The Suzuki coupling reaction[29] of the bromo product **6** with 5-formyl-2-thiopheneboronic acid (**7**) yielded 5-{6-[bis(2′,4′-dihexyloxybiphenyl-4-yl)amino]-8,8-di-methyl-indeno[2,1-b]thiophen-2-yl} thiophene-2-carbaldehyde **8**. The aldehyde compound **8**, upon reaction with cyanoacetic acid in the presence of piperidine, produced the sensitizer JK-306. To further assess the merit of a planar bridging group, we prepared its counterpart JK-305 (see the Supporting Information) by incorporating a dithiophene bridge as a reference.

Spectroscopic studies

The absorption and emission spectra of JK-305 and JK-306 in ethanol are shown in Figure S1. The JK-305 dye with the bithiophene linker has an absorption maximum at 451 nm, which is assigned to the π–π^* transition of the conjugated molecule. Upon using the planar indeno[1,2-*b*]thiophene unit for JK-306, the absorption band is significantly red-shifted to 471 nm. Moreover, the molar absorption coefficient at the maximum absorption band is increased from 3.19×10^4 to $3.46 \times 10^4 \, \text{m}^{-1} \text{cm}^{-1}$ during the π-linker planarization. The bathochromic and hyperchromic effects of introducing a planar indeno[1,2-*b*]thiophene unit into JK-306 can be understood from the molecular-modeling study of the dye. The ground-state configuration of JK-306 possesses a 1.8° twist between the indenothiophene and the adjacent thiophene unit, which resulted in an almost planar configuration. For JK-305, the dihedral angle between the aniline and the thienyl moieties and between two thienyl moieties are 24.6° and 3.2°, respectively, which results in a more twisted configuration compared to its counterpart JK-306. Thus, a high molar extinction coefficient and a significant red-shift of JK-306 relative to JK-305 derive from an increased delocalization over an entire conjugated bridging unit.

Electrochemical properties of these two sensitizers were evaluated by using cyclic voltammetry in acetonitrile with 0.1 m tetrabutylammonium hexafluorophosphate. TiO$_2$ films stained with the sensitizers were used as working electrodes. The oxidation potential of the two sensitizers adsorbed on the TiO$_2$ film shows a quasi-reversible couple at 0.97 and 1.03 V versus standard hydrogen electrode (NHE), respectively. The oxidation potential of JK-305 is less positive than that of JK-306, which indicates an increased electron-donating ability of JK-305 compared with that of JK-306 because of the localization of the amino moiety and the π-linker unit. The reduction potentials of JK-305 and JK-306 calculated from the oxidation potential and the E_{0-0} values determined from the intersection of absorption and emission spectra are listed in Table S1. The excited-state oxidation potentials (E_{ox}) of JK-305 (−1.33 V vs. NHE) and JK-306 (−1.18 V vs. NHE) are more negative than the conduction band of TiO$_2$ (−0.5 V vs. NHE). Thus, the downhill energy offset of the lowest unoccupied molecular orbital (LUMO) in both dyes ensures the thermodynamic driving force for electron injection.[30]

Scheme 1. Schematic diagram for the synthesis of JK-306; i) Pd$_2$(dba)$_3$ (dba = dibenzalacetone), P(*t*Bu)$_3$, *t*BuONa, toluene, reflux; ii) NBS, CH$_2$Cl$_2$, room temperature; iii) Pd(PPh$_3$)$_4$, K$_2$CO$_3$, H$_2$O, THF, reflux; iv) **7**, piperidine, cyanoacetic acid, AcCN, CHCl$_3$, reflux. Full reaction conditions are detailed in the Supporting Information.

Theoretical calculation

We performed the molecular orbital calculation for JK-305 and JK-306 to gain insight into the photophysical properties by using the B3LYP/6-31G(d) method. The isodensity plots of the frontier molecular orbitals of JK-305 and JK-306 are shown in Figure 2. The calculation illustrates that the highest occupied
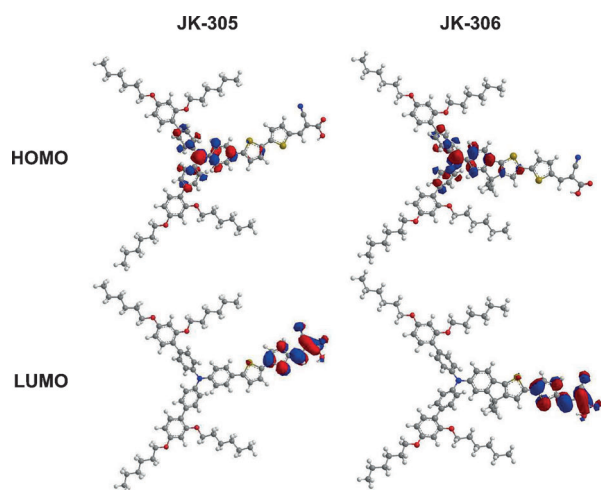

Figure 2. Isodensity surface plots of the HOMO and LUMO of JK-305 and JK-306. The molecular orbital calculation of dyes were performed by using the B3LYP/6-31G(d) method.

molecular orbital (HOMO) of both sensitizers is delocalized over the π-conjugated system through the triphenyl amino group. The LUMO of both sensitizers is delocalized over the cyanoacrylic acid unit with a sizable population on the next thiophene unit. As light excitation should be associated with vectorial electron flow from the HOMO to the LUMO for efficient electron transfer, the examination of HOMO–LUMO of both sensitizers indicates that HOMO–LUMO excitation moved the electron distribution from the triphenylamino moiety to the cyanoacrylic acid group.

Electrochemical impedance spectroscopy

To better understand the improved performance of the JK-306-sensitized solar cell with HC-A instead of CDCA in the Co^{II}/Co^{III} electrolyte system, electrochemical impedance spectroscopy (EIS) measurements were performed on the same devices. The recombination resistance (R_{ct}) and transport resistance (R_t) as well as the capacitance (C_μ) for the JK-306-sensitized cells based on the HC-A and CDCA co-adsorbents in the dark are shown in Figure 3. The respective Nyquist plots are presented in Figure S4. As can be seen, R_{ct} is higher for HC-A than for CDCA in the range of applied forward bias potentials; thus, it is expected that the dark current is lower for HC-A than for CDCA. There was no noticeable difference in C_μ between JK-306 solar cells based on HC-A and CDCA. As shown in Figure 3b, the electron lifetime ($\tau_r = C R_{ct}$)[31] for HC-A was longer than that for CDCA in the range of applied forward bias poten-
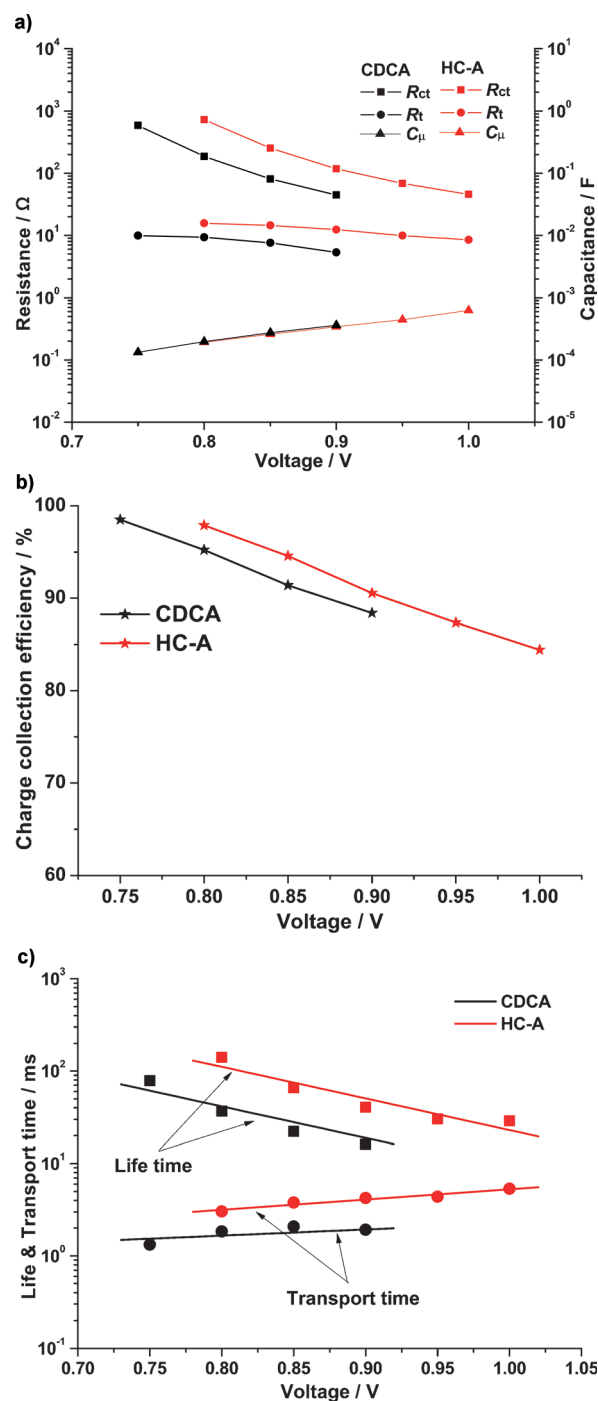

Figure 3. a) R_t, R_{ct}, and C_μ of the JK-306-sensitized cell with CDCA and HC-A as co-adsorbents for the Co^{II}/Co^{III} redox couple under dark conditions. b) Charge collection efficiency of the same devices as a function of applied bias potential. c) The electron lifetime and the transport time for the same devices as a function of forward bias potential.

tials. The co-adsorption of HC-A instead of CDCA, which forms an insulating layer, blocks the recombination of electrons with the [Co(bpy)$_3$]$^{3+}$ (bpy = 2,2′-bipyridine) ions and thus enhances the electron lifetime.[25–27] The longer electron lifetime contributed to a higher open-circuit voltage (V_{oc}). Furthermore, the photovoltaic performance is reflected by the charge collection efficiency (η_{cc}) derived from $\eta_{cc} = (1 + R_t/R_{ct})^{-1}$ or $(1 + \tau_t/\tau_r)^{-1}$.[32]

The η_{cc} for HC-A is higher in the range of forward bias potentials compared to that for CDCA. For the I^-/I_3^- electrolyte system, trends consistent with the aforementioned results were obtained and are presented in Figure S5.

To further investigate the simultaneous improvements in V_{oc} and J_{sc} (short-circuit photocurrent density), the examination of changes in the surface trapping sites were performed by using cyclic voltammetry[33] on each JK-306-sensitized TiO_2 electrode with HC-A and CDCA immersed in 0.1 M $LiClO_4$ in acetonitrile (Figure S6). The capacitive currents of two electrodes at the $TiO_2/LiClO_4$ interface are shown in Figure 4, which demonstrat-
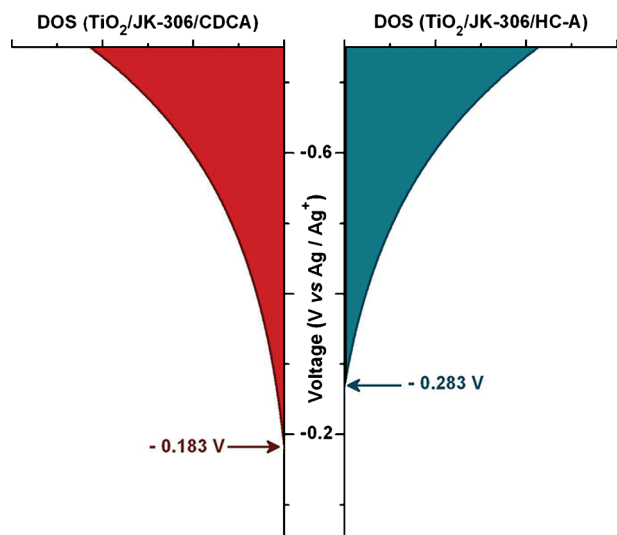

Figure 4. The exponential distribution of DOS was deduced by plotting capacitive charging of electrons in the surface states versus applied potential. The capacitive charging current appearing at a negative potential is attributable to the filling of surface states below the conduction band edge of TiO_2 for all structures.

ed gradual onsets under a forward potential. The distribution of trap states can be estimated from the density of states (DOS) calculation by using $DOS = (dQ/dV)(N_A/F)$,[33] in which Q is the total number of surface trapping sites, N_A Avogadro's number, F Faraday's constant, and V the potential applied to the electrode. As shown in Figure 4, the onsets of the capacitive currents were around −0.183 V for CDCA whereas the TiO_2 electrode covered with JK-306 and HC-A together demonstrated onsets of around −0.283 V, which indicates that the edge of the TiO_2 conduction band moved to lower values (toward the vacuum level). In DSSCs, V_{oc} is determined from the difference between the quasi-Fermi level and the redox potential of redox couple in the electrolyte;[34] therefore, a higher V_{oc} of the JK-306-sensitized cell with HC-A should originate from the negative shift of the quasi-Fermi level of its electrode.

Moreover, dQ/dV of the JK-306-sensitized electrode with HC-A was smaller than that with CDCA. This indicated a reduction in the number of surface trapping sites at which photoinduced electrons could recombine with oxidized species (e.g., $[Co(bpy)_3]^{3+}$).[33] Therefore, we concluded that the multifunctional effects, such as the breakup of dye aggregates, the neg-

ative shift of TiO_2 conduction band edge, and the reduced number of surface trapping sites, contributed simultaneously to improvements in V_{oc} and J_{sc} for the JK-306-sensitized solar cell based on HC-A.

Photovoltaic performance

The spectra of monochromatic incident photon-to-current conversion efficiencies (IPCEs) for DSSCs based on JK-305 and JK-306 with CDCA in combination with an iodine electrolyte are shown in Figure 5. The onset wavelength of the IPCE spectrum for the device based on JK-305 is 720 nm. However, the
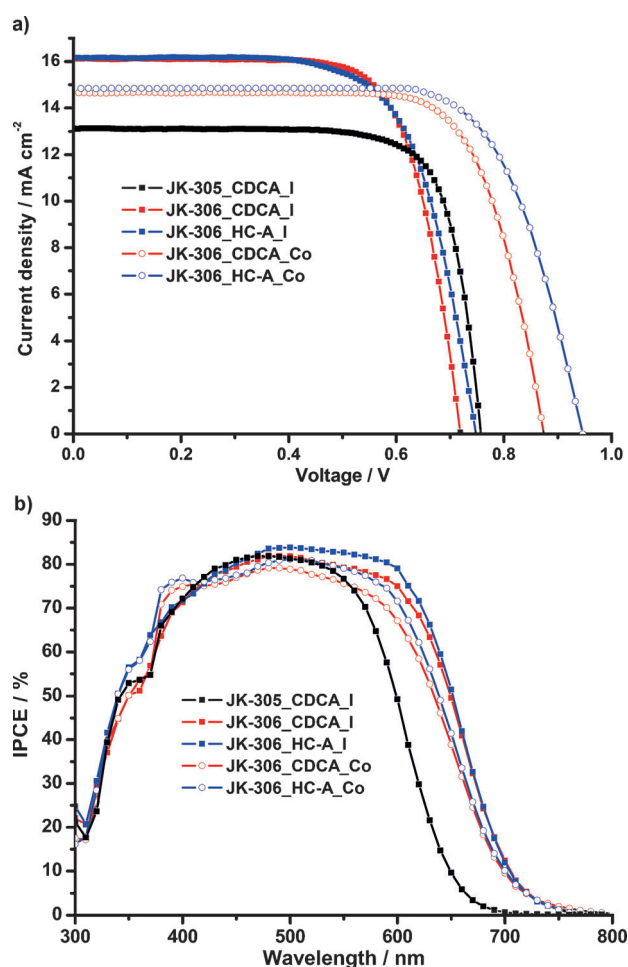

Figure 5. a) Photocurrent–voltage response under simulated full AM 1.5G sunlight using JK-305- and JK-306-sensitized TiO_2 films together with CDCA or HC-A in the presence of the iodine or cobalt electrolyte. b) IPCE as a function of wavelength.

spectrum of JK-306 tails off toward 800 nm, which contributes to the broad spectral light harvesting. The IPCE spectrum of JK-306 is significantly red-shifted by 80 nm compared to that of JK-305, which is consistent with their absorption spectra.

The J–V curve for the JK-305-sensitized cell gave rise to a J_{sc} of 13.12 mA cm^{-2}, a V_{oc} of 0.76 V, and a fill factor (ff) of 0.73, which afforded an overall conversion efficiency (η) of 7.29%.

Under the same conditions, the JK-306-sensitized cell gave rise to a J_{sc} of 14.10 mA cm^{-2}, V_{oc} of 0.75 V, and ff of 0.70, which afforded η of 8.37%. A significant increase in J_{sc} of JK-306 stems from the high molar extinction coefficient and the broad and red-shifted UV spectrum of JK-306 through the delocalization over an entire conjugated system. Upon changing the co-adsorbent from CDCA to HC-A in the JK-306-sensitized cell, the maximum IPCE improved significantly up to 35% at 360 nm compared to that of JK-305, which contributes to the increased photocurrent of the cell. The efficiency of 8.52% in the JK-306-sensitized cell was slightly improved ($J_{sc}=16.14$ mA cm^{-2}, $V_{oc}=0.75$ V, and $ff=0.71$) compared to that of the JK-306-sensitized cell with CDCA, which should be attributed to the role of HC-A having multifunctional effects,[25–27] such as preventing dye aggregation, a light harvesting effect in the shorter wavelength regions around 360 nm, and fast dye regeneration through the hole conducting effect. Moreover, the JK-306 dye exhibits highly efficient photovoltaic performances if the Co^{II}/Co^{III} electrolyte is used instead of the I$^-$/I$_3^-$ electrolyte.

The JK-306-sensitized cell was fabricated with the Co^{II}/Co^{III} electrolyte containing 0.22 M [Co^{II}(bpy)$_3$](B(CN)$_4$)$_2$, 0.05 M [Co^{III}-(bpy)$_3$](B(CN)$_4$)$_3$, 0.1 M LiClO$_4$, and 0.8 M 4-tertbutylpyridine (TBP), in acetonitrile. For CDCA, a high conversion efficiency of 9.40% under simulated sunlight (100 mA cm^{-2}, AM 1.5G) was achieved at $J_{sc}=14.67$ mA cm^{-2}, $V_{oc}=0.87$ V, and $ff=0.71$. Upon the use of HC-A with JK-306, the cell shows a notably improved conversion efficiency of 10.02% with a J_{sc} of 14.33 mA cm^{-2}, V_{oc} of 0.95 V, and ff of 0.71. It is one of the highest values reported for DSSCs with a cobalt-based electrolyte.[32,35] The V_{oc} of 0.95 V based on the cobalt electrolyte and HC-A is 0.2 V higher than for the iodine electrolyte under the same conditions; this results in an overall conversion efficiency increase of approximately 17%. This improved V_{oc} value is attributed to a large energy difference between the TiO$_2$ conduction band and the redox couple of the cobalt electrolyte and suppression of dark current owing to the blocking effect of HC-A. However, the device exhibits a significant decrease in J_{sc} relative to the iodine congener. The slow diffusion of the cobalt-based cell may limit J_{sc} (Figure S2 and Table 1).[36]

The long-term stability is a vital factor for sustained cell operation. Therefore, we substituted the liquid-based electrolyte with a quasi-solid-state one because the cells using the liquid electrolyte have many drawbacks, such as leakage, evaporation, and corrosion of the metals by the I$^-$/I$_3^-$ electrolyte. The photovoltaic performance of JK-305- and JK-306-sensitized cells using a polymer gel electrolyte composed of 5 wt% poly-(vinylidenefluoride-co-hexafluoropropylene), 0.05 M I$_2$, 0.6 M 1,2-dimethyl-3-propyl-imidazolium iodide, 0.1 M LiI, and 0.8 M N-methyl-benzimidazole in acetonitrile is shown in Figure 6. The JK-305-sensitized cell gave rise to a J_{sc} of 12.40 mA cm^{-2}, V_{oc} of 0.74 V, and ff of 0.76, which afforded η of 7.00%. Under the same conditions, the JK-306-sensitized cell gave rise to η of 7.61% with a J_{sc} of 14.02 mA cm^{-2}, V_{oc} of 0.73 V, and ff of 0.74. The conversion efficiency for the JK-306-sensitized cell is approximately 0.61%, which is superior to that of the JK-305-sensitized cell and attributable to a significant improvement in J_{sc}. This result demonstrated a trend similar to that of liquid-

Table 1. Photovoltaic properties of JK-305 and JK-306.						
Dye	Electrolyte	Co-adsorbent	J_{sc} [mA cm^{-2}]	V_{oc} [V]	ff	$\eta^{[a]}$ [%]
JK-305[b]	iodine[c]	CDCA	13.12	0.76	0.73	7.29
JK-306[b]	iodine[c]	CDCA	16.10	0.72	0.70	8.37
JK-306[d]	iodine[c]	HC-A	16.14	0.75	0.71	8.52
JK-306[b]	cobalt[e]	CDCA	14.67	0.87	0.73	9.40
JK-306[d]	cobalt[e]	HC-A	14.83	0.95	0.71	10.02

[a] Irradiated light: AM 1.5G (100 mW cm^{-2}); cell area tested with a metal mask: 0.16 cm^2. [b] Dipping solution: 0.3 mM dye solution (EtOH/THF = 2:1) with 20 mM CDCA. [c] Iodine electrolyte: 0.6 M 1,2-dimethyl-3-propyl-imidazolium iodide, 0.05 M I$_2$, 0.1 M LiI, 0.8 M TBP in AcN. [d] Dipping solution: 0.3 mM dye solution (EtOH/THF=2:1) with 0.3 mM HC-A. [e] Cobalt electrolyte: 0.22 M [Co^{II}(bpy)$_3$](B(CN)$_4$)$_2$, 0.05 M [Co^{III}-(bpy)$_3$](B(CN)$_4$)$_3$, 0.1 M LiClO$_4$, and 0.8 M TBP in AcCN.
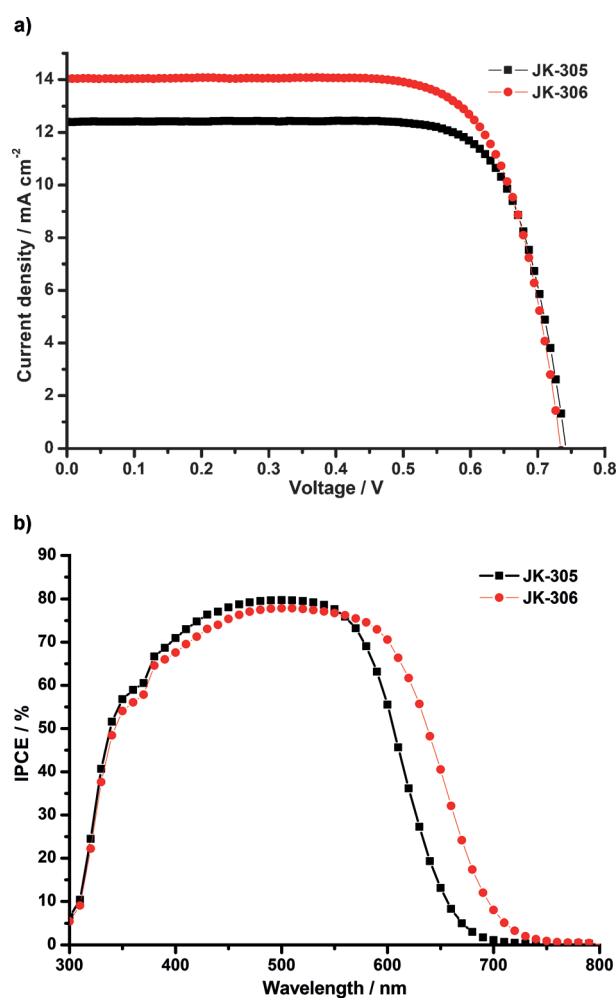

Figure 6. a) J–V curve and b) IPCE spectra of polymer gel-based cells with JK-305 and JK-306. Cell area tested with a metal mask = 0.16 cm^2.

based electrolytes. The efficiency of 7.61% is one of the highest values for a cell based on organic sensitizers.[37,38]

Conclusions

We have designed and synthesized an efficient organic sensitizer (JK-306) with a planar indeno[1,2-*b*]thiophene as a π-linker and a highly congested bulky amino group as an electron donor. The devices based on the JK-306 sensitizer with CDCA and HC-A as co-adsorbents resulted in high conversion efficiencies of 8.37% and 8.52%, respectively. The JK-306-based solar cell fabricated with the Co^{II}/Co^{III} redox couple afforded a significantly improved conversion efficiency of 10.02%, which was attributable to the multifunctional effect, such as the breakup of dye aggregates, the negative shift of TiO_2 conduction band edge, and the reduced number of surface trapping sites attributed to HC-A instead of CDCA. This is one of the highest values reported for DSSCs with cobalt-based electrolytes. Moreover, the JK-306-sensitized solar cell with a polymer gel electrolyte resulted in a high conversion efficiency of 7.61%, which is one of the highest values reported for a cell based on organic sensitizers. We believe that the development of highly efficient organic sensitizers may be possible through meticulous molecular engineering of organic sensitizers.

Experimental Section

The fluorine-doped tin oxide (FTO) glass plates (Pilkington TEC Glass–TEC 8, Solar 2.3 mm thick) were cleaned in a detergent solution by using an ultrasonic bath for 30 min and rinsed with H_2O and EtOH. The FTO glass plates were immersed in $TiCl_4$ (40 mM) at 70 °C for 30 min and washed with H_2O and EtOH. A transparent nanocrystalline layer on the FTO glass plates were prepared through screen printing with the TiO_2 paste (Dyesol, 18NR-T) and then dried at 120 °C. The TiO_2 electrodes were gradually heated under an air flow at 325 °C for 5 min, at 375 °C for 5 min, at 450 °C for 15 min, and at 500 °C for 15 min. A paste for the scattering layer containing 400 nm sized anatase particles (CCIC, PST-400C) was deposited through screen printing and then dried for 1 h at 120 °C. The TiO_2 electrodes were gradually heated under an air flow at 325 °C for 5 min, at 375 °C for 5 min, at 450 °C for 15 min, and at 500 °C for 15 min. The resulting layer was composed of a 6 μm thick transparent layer and a 4 μm thick scattering layer. The TiO_2 electrodes were again treated with $TiCl_4$ at 70 °C for 30 min and sintered at 500 °C for 30 min. The TiO_2 electrodes were immersed in the dye solution (0.3 mM in THF/EtOH = 1:2 containing 20 mM CDCA or 0.3 mM HC-A) and kept at room temperature for 12 h. Then, the Pt on FTO plates as counter electrodes was cleaned in an ultrasonic bath in H_2O, acetone, and HCl (2 M, aqueous). The counter electrodes were prepared by coating with a drop of the H_2PtCl_6 solution (2 mg of Pt in 1 mL of EtOH) on an FTO plate and heating at 400 °C for 15 min. The dye adsorbed on the TiO_2 electrode and the Pt-counter electrode were assembled into a sealed sandwich-type cell by heating at 80 °C with a hot-melt film (60 μm thick Surlyn) as a spacer between the electrodes. A drop of the electrolyte solution was placed on a drilled hole in the counter electrode of the assembled cell and was driven into the cell through vacuum backfilling. Finally, the hole was sealed by using additional Surlyn and a cover glass (0.1 mm thick).

Acknowledgements

[1] B. O'Regan, M. Grätzel, *Nature* **1991**, *353*, 737.
[2] M. Grätzel, *Nature* **2001**, *414*, 338–344.
[3] M. K. Nazeeruddin, F. De Angelis, S. Fantacci, A. Selloni, G. Viscardi, P. Liska, S. Ito, T. Bessho, M. Grätzel, *J. Am. Chem. Soc.* **2005**, *127*, 16835–16847.
[4] M. Grätzel, *Prog. Photovoltaics* **2006**, *14*, 429–442.
[5] J. Tang, W. Wu, J. Hua, J. Li, X. Li, H. Tian, *Energy Environ. Sci.* **2009**, *2*, 982–990.
[6] A. Abbotto, N. Manfredi, C. Marinzi, F. D. Angelis, E. Mosconi, J.-H. Yum, Z. Xianxi, M. K. Nazeeruddin, M. Grätzel, *Energy Environ. Sci.* **2009**, *2*, 1094–1101.
[7] J. N. Clifford, E. Palomares, M. K. Nazeeruddin, M. Grätzel, J. Nelson, X. Li, N. J. Long, J. R. Durrant, *J. Am. Chem. Soc.* **2004**, *126*, 5225–5233.
[8] C. S. Karthikeyan, H. Wietasch, M. Thelakkat, *Adv. Mater.* **2007**, *19*, 1091–1095.
[9] S. A. Haque, S. Handa, K. Peter, E. Palomares, M. Thelakkat, J. R. Durrant, *Angew. Chem.* **2005**, *117*, 5886–5890; *Angew. Chem. Int. Ed.* **2005**, *44*, 5740–5744.
[10] H. Choi, S. O. Kang, J. Ko, G. Gao, H. S. Kang, M.-S. Kang, M. K. Nazeeruddin, M. Grätzel, *Angew. Chem.* **2009**, *121*, 6052–6055; *Angew. Chem. Int. Ed.* **2009**, *48*, 5938–5941.
[11] K. Do, D. Kim, N. Cho, S. Paek, K. Song, J. Ko, *Org. Lett.* **2012**, *14*, 222–225.
[12] P. Wang, S. M. Zakeeruddin, P. Comte, R. Charvet, R. Humphry-Baker, M. Grätzel, J. Phys. Chem. B **2003**, *107*, 14336–14341.
[13] Y. Bai, J. Zhang, D. Zhou, Y. Wang, M. Zhang, P. Wang, *J. Am. Chem. Soc.* **2011**, *133*, 11442–11445.
[14] H. N. Tsao, C. Yi, T. Moehl, J.-H. Yum, S. M. Zakeeruddin, M. K. Nazeeruddin, M. Grätzel, *ChemSusChem* **2011**, *4*, 591–594.
[15] N. Cai, S.-J. Moon, L. Cevey-Ha, T. Moehl, R. Humphy-Baker, P. Wang, S. M. Zakeeruddin, M. Grätzel, *Nano Lett.* **2011**, *11*, 1452–1456.
[16] S. Ko, H. Choi, M.-S. Kang, H. Hwang, H. Ji, J. Kim, J. Ko, Y. Kang, *J. Mater. Chem.* **2010**, *20*, 2391–2399.
[17] L.-Y. Lin, C.-H. Tsai, K.-T. Wong, T.-W. Huang, L. Hsieh, S.-H. Liu, H.-W. Lin, C.-C. Wu, S.-H. Chou, S.-H. Chen, *J. Org. Chem.* **2010**, *75*, 4778–4785.
[18] X. Zhu, H. Tsuji, A. Yella, A.-S. Chauvin, M. Grätzel, E. Nakamura, *Chem. Commun.* **2013**, *49*, 582–584.
[19] J.-H. Chen, C.-H. Tsai, S.-A. Wang, Y.-Y. Lin, T.-W. Huang, S.-F. Chiu, C.-C. Wu, K.-T. Wong, *J. Org. Chem.* **2011**, *76*, 8977–8985.
[20] N. Cai, R. Li, Y. Wang, M. Zhang, P. Wang, *Energy Environ. Sci.* **2013**, *6*, 139–147.
[21] K. Lim, C. Kim, J. Song, T. Yu, W. Lim, K. Song, P. Wang, N. Zu, J. Ko, *J. Phys. Chem. C* **2011**, *115*, 22640–22646.
[22] P. H. Mutin, G. Guerrero, A. Vioux, *J. Mater. Chem.* **2005**, *15*, 3761–3768.
[23] M. Wang, X. Li, H. Lin, P. Pechy, S. M. Zakeeruddin, M. Grätzel, *Dalton Trans.* **2009**, 10015–10020.
[24] T. Marinado, M. Hahlin, X. Jiang, M. Quintana, E. M. J. Johansson, E. Gabrielsson, S. Plogmaker, D. P. Hagberg, G. Boschloo, S. M. Zakeeruddin, M. Grätzel, H. Siegbahn, L. Sun, A. Hagfeldt, H. Rensmo, *J. Phys. Chem. C* **2010**, *114*, 11903–11910.

[25] B. J. Song, H. M. Song, I. T. Choi, S. K. Kim, K. D. Seo, M. S. Kang, M. J. Lee, D. Cho, M. J. Ju, H. K. Kim, *Chem. Eur. J.* **2011**, *17*, 11115 – 11121.

[26] M. S. Kang, S. H. Kang, S. K. Kim, I. T. Choi, J. H. Ryu, M. J. Ju, D. Cho, J. Y. Lee, H. K. Kim, *Chem. Commun.* **2012**, *48*, 9349 – 9351.

[27] S. H. Kang, I. T. Choi, M. S. Kang, Y. K. Eom, M. J. Ju, J. Y. Hong, H. S. Kang, H. K. Kim, *J. Mater. Chem. A* **2013**, *1*, 3977 – 3982.

[28] N. Cho, H. Choi, D. Kim, K. Song, M.-S. Kang, S. O. Kang, J. Ko, *Tetrahedron* **2009**, *65*, 6236 – 6243.

[29] C.-H. Huang, N. D. McClenaghan, A. Kuhn, J. W. Hofstraat, D. M. Bassani, *Org. Lett.* **2005**, *7*, 3409 – 3412.

[30] A. Hagfeldt, M. Grätzel, *Chem. Rev.* **1995**, *95*, 49 – 68.

[31] E. M. Barea, J. Ortiz, F. J. Payá, F. Fernández-Lázaro, F. Fabregat-Santiago, A. Sastre-Santos, J. Bisquert, *Energy Environ. Sci.* **2010**, *3*, 1985 – 1994.

[32] J.-H. Yum, E. Baranoff, F. Kessler, T. Moehl, S. Ahmad, T. Bessho, A. Marchioro, E. Ghadiri, J.-E. Moser, C. Yi, M. K. Nazeeruddin, M. Grätzel, *Nat. Commun.* **2012**, *3*, 631.

[33] Z. Zhang, S. M. Zakeeruddin, B. O'Regan, R. Humphry-Baker, M. Grätzel, *J. Phys. Chem. B* **2005**, *109*, 21818 – 21824.

[34] L. M. Peter, N. W. Duffy, R. L. Wang, K. G. U. Wijayantha, *J. Electroanal. Chem.* **2002**, *524*, 127 – 136.

[35] H. N. Tsao, J. Burschka, C. Yi, F. Kessler, M. K. Nazeeruddin, M. Grätzel, *Energy Environ. Sci.* **2011**, *4*, 4921 – 4924.

[36] H. Nusbaumer, S. M. Zakeeruddin, J.-E. Moser, M. Grätzel, *Chem. Eur. J.* **2003**, *9*, 3756 – 3763.

[37] S. Kim, D. Kim, H. Choi, M.-S. Kang, K. Song, S. O. Kang, J. Ko, *Chem. Commun.* **2008**, 4951 – 4953.

[38] J.-J. Kim, H. Choi, J.-W. Lee, M.-S. Kang, K. Song, S. O. Kang, J. Ko, *J. Mater. Chem.* **2008**, *18*, 5223 – 5229.